Protein Science (1994), *3*:1547–1555. Cambridge University Press. Printed in the USA.

Facile transition between 3_{10}- and α-helix: Structures of 8-, 9-, and 10-residue peptides containing the -(Leu-Aib-Ala)$_2$-Phe-Aib- fragment

ISABELLA L. KARLE,[1] JUDITH L. FLIPPEN-ANDERSON,[1] R. GURUNATH,[2] AND P. BALARAM[2]

[1] Laboratory for the Structure of Matter, Naval Research Laboratory, Washington, D.C. 20375-5320
[2] Molecular Biophysics Unit, Indian Institute of Science, Bangalore 560 012, India

(RECEIVED March 15, 1994, ACCEPTED June 13, 1994)

Abstract

A structural transition from a 3_{10}-helix to an α-helix has been characterized at high resolution for an octapeptide segment located in 3 different sequences. Three synthetic peptides, decapeptide (A) Boc-Aib-Trp-(Leu-Aib-Ala)$_2$-Phe-Aib-OMe, nonapeptide (B) Boc-Trp-(Leu-Aib-Ala)$_2$-Phe-Aib-OMe, and octapeptide (C) Boc-(Leu-Aib-Ala)$_2$-Phe-Aib-OMe, are completely helical in their respective crystals. At 0.9 Å resolution, *R* factors for A, B, and C are 8.3%, 5.4%, and 7.3%, respectively. The octapeptide and nonapeptide form ideal 3_{10}-helices with average torsional angles ϕ(N–C$^\alpha$) and ψ(C$^\alpha$–C′) of −57°, −26° for C and −60°, −27° for B. The 10-residue peptide (A) begins as a 3_{10}-helix and abruptly changes to an α-helix at carbonyl O(3), which is the acceptor for both a 4 → 1 hydrogen bond with N(6)H and a 5 → 1 hydrogen with N(7)H, even though the last 8 residues have the same sequence in all 3 peptides. The average ϕ,ψ angles in the decapeptide are −58°, −28° for residues 1–3 and −63°, −41° for residues 4–10. The packing of helices in the crystals does not provide any obvious reason for the transition in helix type. Fourier transform infrared studies in the solid state also provide evidence for a 3_{10}- to α-helix transition with the amide I band appearing at 1,656–1,657 cm^{-1} in the 9- and 10-residue peptides, whereas in shorter sequences the band is observed at 1,667 cm^{-1}.

Keywords: α-aminoisobutyric acid peptides; helical peptide structures; helical transitions; helix packing; peptide conformation

The α-helix is a widely characterized structural element in proteins, whereas the closely related 3_{10}-helix is much less frequently found (Barlow & Thornton, 1988). However, 3_{10}-helices have been extensively documented in peptides containing α-aminoisobutyric acid, Aib (Francis et al., 1983; Prasad & Balaram, 1984; Karle, 1992), with as many as 3 to 4 turns of 3_{10}-helical conformations observed in crystal structures (Karle & Balaram, 1990; Toniolo & Benedetti, 1991). Complete 3_{10}-helices are found in homo-oligopeptides of Aib (Pavone et al., 1990a) with mixed $3_{10}/\alpha$-helical structures being detected in heteromeric sequences (Karle & Balaram, 1990). More recently, 3_{10}-helical conformations have been proposed for 16–17-residue alanine-rich peptides in aqueous solutions, based on electron spin resonance spectra of doubly labeled helices (Miick et al., 1992; Fiori et al., 1993). 3_{10}- to α-helical transitions may be important in accommodation of mutational insertions into protein helices as noted for hemoglobin Catonsville (Kavanaugh et al., 1993). Further, helix distortion by insertion has also been established in staphylococcal nuclease (Keefe et al., 1993). The character of 3_{10}- to α-helical transitions is thus of interest, particularly with respect to establishing chain length and sequence dependencies. Short helical sequences afford the possibility of observing such transitions at high structural resolution.

In the case of Aib-containing peptides, sequences with 5 residues or less form 3_{10}-helices or incipient 3_{10}-helices (Prasad & Balaram, 1984). Those with more than 10 residues prefer to form mixed 3_{10}-/α-, or α-helices (Karle & Balaram, 1990). Figure 1 shows the relationship between helix type as a function of the number of Aib residues with respect to the total number of residues in a peptide (Karle & Balaram, 1990; Karle, 1992). The information for the graph has been obtained from well-determined crystal structures with resolutions of ~0.9 Å. Near the arbitrarily drawn boundary separating 3_{10}- and α-helices, the helix types for several peptides are "misplaced" and indicate that the transition between 3_{10}- and α-helix types is rather fac-

Reprint requests to: Isabella L. Karle, Laboratory for the Structure of Matter, Code 6030, Naval Research Laboratory, Washington, D.C. 20375-5320, or P. Balaram, Molecular Biophysics Unit, Indian Institute of Science, Bangalore 560 012, India.

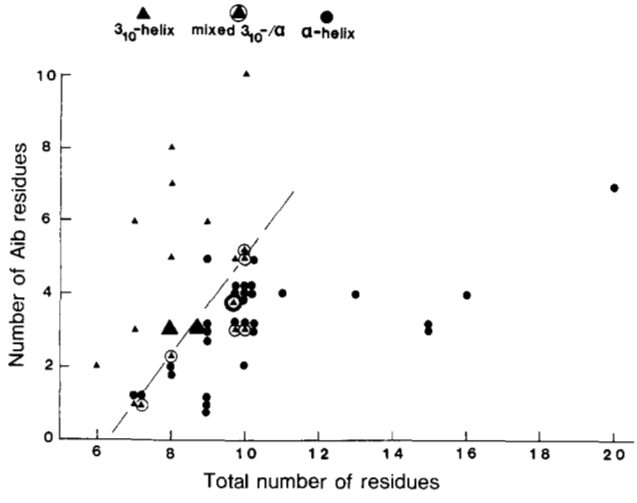

Fig. 1. Graph showing the occurrence of 3_{10}-, mixed 3_{10}-/α-, and α-helices in crystalline apolar peptides having 6 or more residues. The quantities plotted are the number of Aib residues versus the total number of residues in a peptide. The enlarged symbols represent the location of the 3 peptides discussed in this paper. Different peptides that would fall in the same location are slightly offset from each other. The dashed line shows an approximate boundary between 3_{10}- and α-helices.

ile and isoenergetic. The somewhat indefinite boundary also suggests that additional subtle factors are involved in determining helix types (Marshall et al., 1990).

The purpose of this investigation was to study the helix types in 3 closely related peptides: Boc-Aib-Trp-(Leu-Aib-Ala)$_2$-Phe-Aib-OMe (A), Boc-Trp-(Leu-Aib-Ala)$_2$-Phe-Aib-OMe (B), and Boc-(Leu-Aib-Ala)$_2$-Phe-Aib-OMe (C), each peptide containing the same 8-residue peptide segment present in C. Trp is inserted at the N-terminus in B, and Aib-Trp is inserted in A (Fig. 2). The locations of these 3 peptides in Figure 1 are emphasized by large symbols. The peptide sequences were synthesized as part of a program to examine helix packing in sequences containing aromatic side chains. The 7-residue separation between Phe and Trp residues was chosen to facilitate "knobs in holes" packing of adjacent helices (Karle et al., 1990a). The crystal structures described in this report establish a facile transition between 3_{10}- and α-helical structures.

Results

The conformations of A, B, and C are shown in Kinemage 1 and in Figure 3A, B, and C, respectively. The 3 molecules are drawn

A: Boc-Aib^1-Trp^2-Leu^3-Aib^4-Ala^5-Leu^6-Aib^7-Ala^8-Phe^9-Aib^{10}-OMe

B: Boc- Trp^2-Leu^3-Aib^4-Ala^5-Leu^6-Aib^7-Ala^8-Phe^9-Aib^{10}-OMe

C: Boc- Leu^3-Aib^4-Ala^5-Leu^6-Aib^7-Ala^8-Phe^9-Aib^{10}-OMe

Fig. 2. Sequence and numbering for peptides A, B, and C. Note that the residues 1 and 2 do not exist in C and residue 1 does not exist in B.

so that the Aib(4)-Ala(5) sequence has the same orientation in each. The conformational angles for the 3 molecules are listed in Table 1 and the hydrogen bond parameters are shown in Tables 2–4.[3]

Peptide C has 6 3_{10}-type NH···OC hydrogen bonds with average values of $-57.5°$ and $-26.4°$ for ϕ and ψ torsional angles, consistent with a 3_{10}-helix. The insertion of the Trp residue between the Boc end group and Leu(3) in C yields the nonapeptide B, which also has a 3_{10}-helix that is almost identical to the helix in C. The additional residue allows an additional 3_{10}-type hydrogen bond at the N-terminus. The largest difference between the backbones in B and C occurs with a greater helix distortion in B than C helix at the penultimate residue where $\phi = -150°$ and $-96°$, respectively. In helices ending with an Aib residue, there often are helix distortions or reversals at the penultimate residue (see, for example, Karle et al., 1986, 1990a), and these appear to be independent of helix length. If residues 9 and 10 are omitted, the average values for ϕ and ψ in B, $-60.2°$ and $-26.7°$, respectively, are quite similar to those in C.

The decapeptide A has been derived from peptide B by the insertion of an Aib residue between Boc and Trp(2) in peptide B. Addition of the Aib residue, of course, lengthens the sequence, a factor that favors the formation of an α-helix. On the other hand, Aib residues have a strong tendency for forming the 3_{10}-helix. In decapeptide A (Fig. 3A; Kinemage 1), the helix begins with 3_{10}-type hydrogen bonds between CO(Boc)···HN(Leu(3)), CO(Aib(1))···HN(Aib(4)), and CO(Trp(2))···HN(Ala(5)). The carbonyl oxygen in Leu(3) is the recipient of 2 hydrogen bonds, 1 from HN(Leu 6) that forms a 3_{10}-type ($4 \rightarrow 1$) and 1 from HN(Aib 7) that forms an α-type ($5 \rightarrow 1$). The $5 \rightarrow 1$ bond is quite normal, whereas the $4 \rightarrow 1$ bond is distorted with respect to the long H···O distance and the small C···O···N angle. A transition between a 3_{10}-helix and an α-helix takes place at this point. All the remaining hydrogen bonds in the helix are the α-type. A stereo diagram of A is shown in Figure 4, with the transition region emphasized (see also Kinemage 1).

In the decapeptide A, the upper part of the helix is a 3_{10}-type where ϕ and ψ average values for residues 1–3 are $-58°$ and $-27.6°$, whereas the remainder of the helix is an α-type where the ϕ and ψ average values for residues 4–10 are $-63°$ and $-41.5°$. None of the ϕ and ψ values for the individual residues in the 3_{10}-helix and the α-helix regions are unusual for that particular helix type, except for the $4 \rightarrow 1$ bond at the point of transition. The plots of ϕ values for the individual residues in molecules A, B, and C are superimposed in Figure 5, as well as the plots for ψ values. The sequences of ϕ values for A, B, and C have quite similar oscillations about $\phi \sim -60°$, with values of $\sim -50°$ for Aib residues in positions 4, 7, and 10. The only aberration is at Phe(9) for peptides B and C, but not for A. Except at Phe(9), the ϕ values for A in the region of the α-helix are several degrees larger than those for B and C, which have a 3_{10}-helix for the same sequence of residues. The ψ plots for B and C are quite similar and oscillate about $\psi \sim -25°$ (except near the C-termini). However, the ψ values for A change from $-21°$ to $-33°$ in the initial 3_{10}-helical region to an oscillation

[3] Supplementary material consisting of bond lengths and angles, anisotropic thermal parameters, and coordinates for H atoms is deposited in the Cambridge Crystallographic Data File. Observed and calculated structure factors are available from I.L.K. and J.L.F.-A.

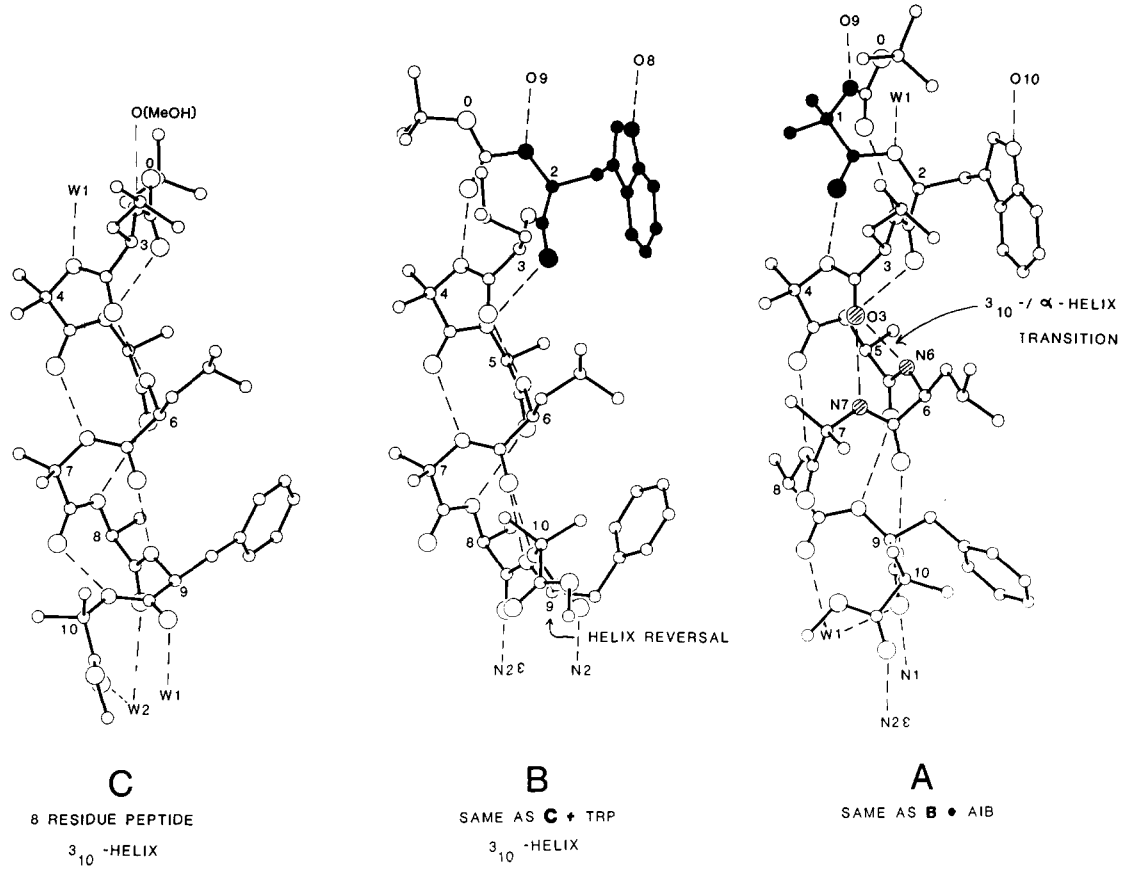

Fig. 3. **C:** The 8-residue peptide Boc-(Leu-Aib-Ala)$_2$-Phe-Aib-OMe in a 3_{10}-helix. Note that the numbering of residues starts at 3 near the N-terminus. **B:** The 9-residue peptide with Trp(2) residue at the N-terminus in a 3_{10}-helix. The numbering of residues starts at 2. **A:** The 10-residue peptide with an Aib(1) residue inserted near the N-terminus. The helix begins as a 3_{10}-type at the N-terminus and changes to an α-type at the O(3)···HN(7) hydrogen bond. The dashed lines indicate intra- and interhelical hydrogen bonds.

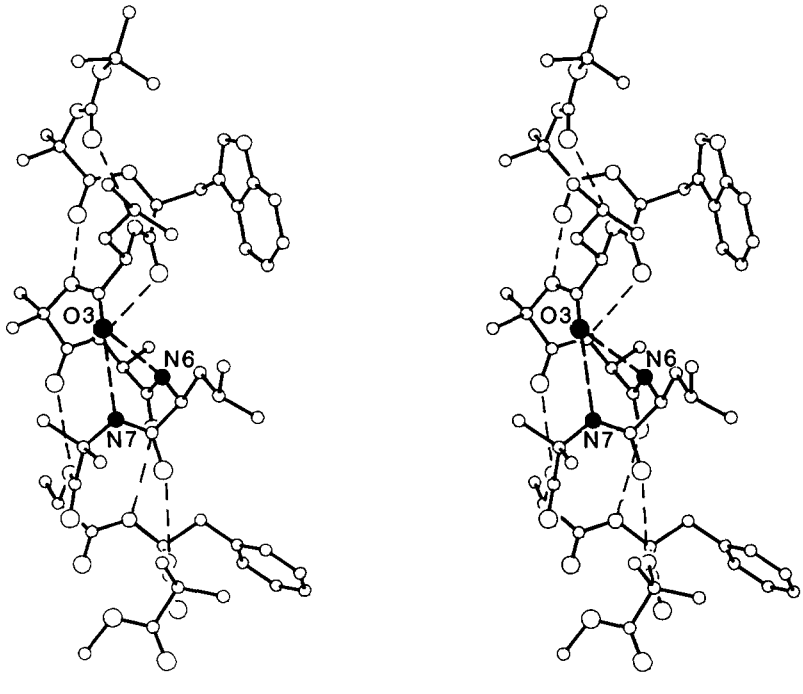

Fig. 4. Stereo diagram of decapeptide A. The transition region from a 3_{10}-helix to an α-helix is shown at O(3), N(6), and N(7) with the two hydrogen bonds to O(3) emphasized by heavy dashed lines.

Table 1. *Torsional angles[a] (deg) in peptides A, B, and C*

Angle (ϕ, ψ, ω) or side chain (χ^1, χ^2)		C	B	A
Aib(1)	ϕ			−63[b]
	ψ			−21
	ω			−178
Trp(2)	ϕ		−62[b]	−58
	ψ		−31	−29
	ω		−178	180
Leu(3)	ϕ	−54[b]	−58	−53
	ψ	−37	−27	−33
	ω	−179	179	−176
Aib(4)	ϕ	−50	−54	−56
	ψ	−32	−33	−45
	ω	−177	−176	−176
Ala(5)	ϕ	−60	−67	−70
	ψ	−23	−20	−32
	ω	−179	176	171
Leu(6)	ϕ	−69	−63	−64
	ψ	−13	−19	−49
	ω	−171	177	−178
Aib(7)	ϕ	−51	−51	−55
	ψ	−31	−32	−46
	ω	−179	−174	−175
Ala(8)	ϕ	−61	−67	−72
	ψ	−22	−25	−24
	ω	−179	−173	175
Phe(9)	ϕ	−96	−150	−77
	ψ	10	5	−47
	ω	176	−173	−174
Aib(10)	ϕ	−49	−50	−47
	ψ	139[c]	137[c]	−48[c]
	ω	−178[d]	174[d]	−176[d]
Trp(2)	χ^1		68	76
	χ^2		−98, 83	−102, 84
Leu(3)	χ^1	−71	−76, (85)[e]	−71
	χ^2	175, −63	−62, 172 (−82, 164)[e]	168, −64
Leu(6)	χ^1	−64	−69	173
	χ^2	177, −60	−69, 167	71, −161
Phe(9)	χ^1	−51	63	179
	χ^2	145, −36	−84, 93	−102, 78
Average	ϕ	−57.5[f]	−60.2[g]	−58.0 (1-3)[h]
				−63.0 (4-10)
Average	ψ (3_{10})	−26.4	−26.7	−27.6 (1-3)
	(α)			−41.5 (4-10)
Aib/total		3/8	3/9	4/10

[a] The torsional angles for rotation about bonds of the peptide backbone (ϕ, ψ, ω) and about bonds of the amino acid side chains (χ^1, χ^2) as suggested by the IUPAC-IUB Commission on Biochemical Nomenclature (1970). Estimated standard deviations ~1.0°.
[b] C′(0), N(i), Cα(i), C′(i).
[c] N(10), Cα(10), C′(10), O(OMe).
[e] Side chain disordered among 2 positions.
[f] Averages for residues 3-8.
[g] Averages for residues 2-8.
[h] Averages for residues 1-3 and 4-10 for the separate 3_{10}- and α-helix regions.

about $\psi \sim -40°$ where the α-helix occurs. It is interesting to note that the same 8-residue segment, which is in a 3_{10}-helix in peptides B and C, becomes an α-helix in peptide A. The only portion of peptide A that has the 3_{10}-helix is the N-terminus

Table 2. *Hydrogen bonds in crystal C*

Type	Donor	Acceptor	(O···O) N···O (Å)	H···O (Å)[a]	C···N[b] angle (deg)
Helix-solvent	N(3)	M(3)[c]	3.11	2.24	
	N(4)	W(1)	2.85	2.10	
4 → 1	N(5)	O(0)	3.01	2.15	128
	N(6)	O(3)	2.94	2.09	130
	N(7)	O(4)	3.01	2.16	125
	N(8)	O(5)	3.16	2.29	124
	N(9)	O(6)	2.88	2.01	126
	N(10)	O(7)	3.03	2.16	121
Solvent-helix or solvent	W(1)	O(9)[d]	2.82		
	W(1)	M(3)[c]	2.79		
	W(2)	O(8)[e]	2.77		
	W(2)	O(10)[e]	2.77		
	M(3)[b]	W(2)	2.61		

[a] Hydrogen atoms placed in idealized positions with N-H = 0.96 Å and X-N-H angles near 120°.
[b] The C=O···N angle.
[c] O atom in methanol solvent molecule.
[d] Symmetry operation 1 + x, y, z for coordinates.
[e] Symmetry operation 1 + x, −1 + y, z for coordinates.

containing the Boc end group and the added residues Aib and Trp, followed by the original initial residue Leu. The easy transformation from a 3_{10}-helix to an α-helix is independent of sequence and appears to be a consequence of lengthening the sequence. Any possible influence of crystal packing on helix type is discussed in the next section.

Crystal packing

Head-to-tail hydrogen bonding

Helical peptides (with more than 6 residues) in crystals have almost always been observed to pack in a head-to-tail motif that results in forming long rods or columns of helices throughout the crystal (Bosch et al., 1985a, 1985b; Francis et al., 1985; Karle & Balaram, 1990; Marshall et al., 1990). In crystals where the succeeding α-helices in a column are in good register with respect to each other, 3 intermolecular NH···OC hydrogen bonds can be formed between the head of one helix and the tail of another (Karle et al., 1989, 1992a). In other crystals where succeeding peptides with 3_{10}- or α-helices are not in good register, only 1 intermolecular NH···OC hydrogen bond may form, augmented by water or alcohol molecules that mediate hydrogen bonds between those CO and NH groups that are placed too far apart for direct hydrogen bond formation (Karle et al., 1992b).

In the present paper, crystal C represents the rare case in which there are no direct NH···OC bonds in the head-to-tail region. Furthermore, a polar solvent layer consisting of water-methanol-water groups is formed in the head-to-tail region between the hydrophobic helices (Fig. 6). The N(3)H moiety is a donor to the O atom of a methanol molecule (M), which in turn is an acceptor for a hydrogen bond from water W(1) and a donor to the oxygen of water W(2). Water W(1) is also an accep-

Table 3. *Hydrogen bonds in crystal B*

Type	Donor	Acceptor	(O···O) N···O (Å)	H···O (Å)[a]	C···N[b] angle (deg)
Head-to-tail	N(2)	O(9)[c]	3.04	2.17	108
4 → 1	N(3)				
	N(4)	O(0)	3.06	2.22	132
	N(5)	O(2)	3.03	2.19	129
	N(6)	O(3)	2.98	2.15	123
	N(7)	O(4)	3.08	2.22	125
	N(8)	O(5)	3.15	2.26	124
	N(9)	O(6)	3.08	2.21	127
	N(10)	O(6)	2.83	2.10	174
Head-to-tail	N(2ε)	O(8)[d]	2.83	1.94	153

[a] Hydrogen atoms placed in idealized positions with N-H = 0.96 Å and X-N-H angles near 120°.
[b] The C=O···N angle.
[c] Symmetry operation $-1 + x$, y, $1 + z$ for coordinates.
[d] Symmetry operation $-1 + x$, $-1 + y$, $1 + z$ for coordinates.

tor from N(4) and a donor to carbonyl O(9) of the lower right peptide as shown in Figure 6. Water W(2), an acceptor of a hydrogen bond from the methanol molecule, is a donor to both carbonyl O(8) and carbonyl O(10) of the lower left peptide molecule, as shown in Figure 6. The hydrogen bonding in crystal C connects the helical molecule into a 2-dimensional network rather than a 1-dimensional column.

Crystal B does not contain any solvent molecules (Fig. 7). There are direct NH···OC head-to-tail hydrogen bonds between N(2)H and carbonyl O(9) and between N$^{\epsilon}$(2) of the Trp(2) side chain and carbonyl O(8). The N(3)H moiety does not partici-

Table 4. *Hydrogen bonds in crystal A*

Type	Donor	Acceptor	(O···O) N···O (Å)	H···O (Å)[a]	C···N[b] angle (deg)
Head-to-tail	N(1)	O(9)[c]	2.95	2.10	142
	N(2)	W(1)	3.07	2.25	
4 → 1	N(3)	O(0)	3.29	2.41	128
	N(4)	O(1)	2.97	2.11	128
	N(5)	O(2)	3.05	2.32	124
	N(6)	O(3)	3.15	*2.66*	*109*
5 → 1	N(7)	O(3)	2.98	2.10	162
	N(8)	O(4)	3.16	2.32	146
	N(9)	O(5)	3.22	2.49	145
	N(10)	O(6)	3.03	2.15	166
Head-to-tail	W(1)	O(8)[d]	2.77		
	W(1)	O(9)[d]	2.97		
	N(2ε)	O(10)[e]	3.00	2.30	160

[a] Hydrogen atoms placed in idealized positions with N-H = 0.96 Å and X-N-H angles near 120°.
[b] The C=O···N angle.
[c] Symmetry operation $1.5 - x$, $1 - y$, $0.5 + z$.
[d] Symmetry operation $1.5 - x$, $1 - y$, $-0.5 + z$.
[e] Symmetry operation $2.5 - x$, $1 - y$, $0.5 + z$.

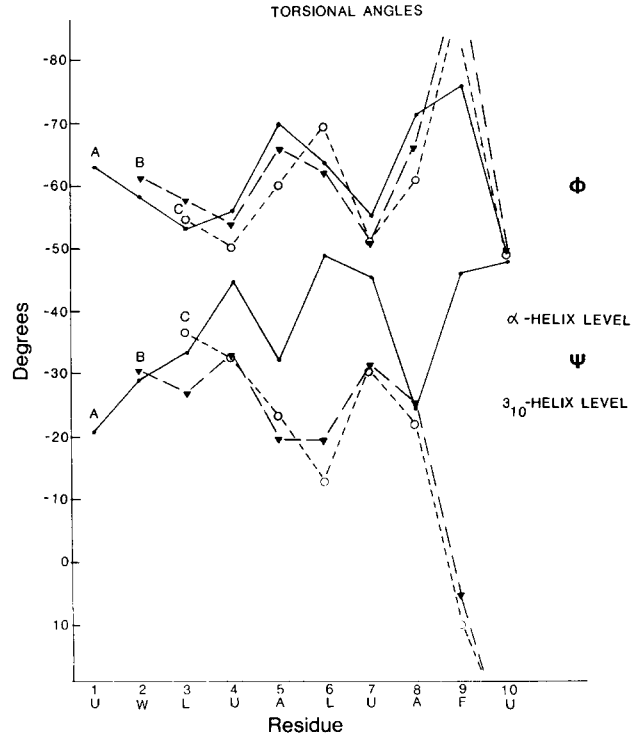

Fig. 5. Superposed plots of ϕ (torsion about N-C$^{\alpha}$) and ψ (torsion about C$^{\alpha}$-C′) values for each residue in peptides A (solid line), B (long dash), and C (short dash).

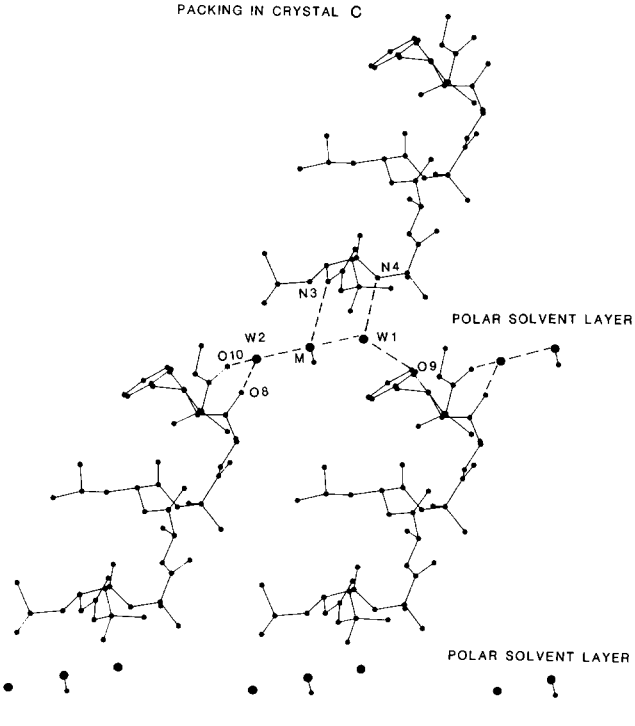

Fig. 6. A layer of molecules in crystal C showing solvent molecules separating the head and the tail regions of the helices. The layers of helices above and below the one shown have their helix axes pointed in opposite direction, i.e., antiparallel packing of helices.

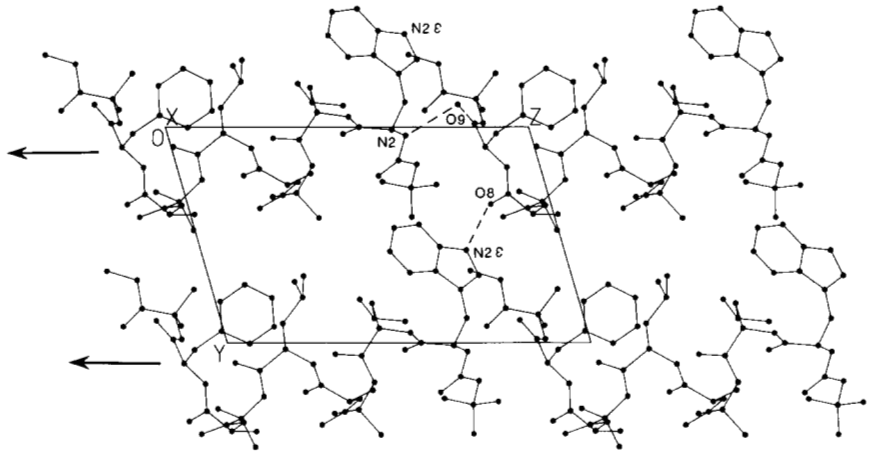

Fig. 7. Packing of 4 molecules in crystal B. Because the peptide B has crystallized with only 1 molecule per cell in space group P1, the packing of helices must be completely parallel.

pate in any hydrogen bond formation, a situation that is found fairly frequently.

Crystal A has a direct N(1)···O(9) head-to-tail hydrogen bond between the helix backbones, a direct $N^{\epsilon}(2)H\cdots O(10)$ bond that involves the Trp(2) side chain, and a water molecule W(1) that mediates hydrogen bonds between N(2)H and carbonyls O(8) and O(9) (Fig. 8). In crystal A (space group $P2_12_12_1$), succeeding alternate molecules in the column formed by hydrogen bonding are related by a 2-fold screw. In crystals B and C, succeeding molecules in a column are related by translation.

Parallel and antiparallel aggregation of helices

The packing arrangements in crystals A, B, and C represent both the case in which all helices are aligned parallel to each other and the case in which helices align in an antiparallel motif, despite the fact that a sequence of 8 residues is the same in the 3 crystals. The preponderance of antiparallel alignment of helices in protein molecules (Richardson, 1981) has been justified by the dipole moment associated with the helix axis (Wada, 1976; Hol et al., 1981; Hol & de Maeyer, 1984). The dipole moment, however, cannot be a determining factor in selecting the direction of helix alignment. For helices composed entirely of apolar residues, many crystals have completely parallel packing of helices. Even peptides with identical sequences that crystallize in more than 1 crystal form will have a parallel assembly in one crystal form and an antiparallel assembly in another crystal form (Karle et al., 1990a, 1990b).

Exact parallel packings of helices in crystals are dictated only when adjacent molecules are related by a translation of 1 cell length, as in space group P1, for example, if there is only 1 molecule per cell. Approximate parallel packing can occur if more than 1 molecule crystallizes per asymmetric unit. Antiparallel packing is more or less exact or skewed depending upon how close to perpendicular the helix axis is to a crystallographic 2-fold screw axis. In apolar helices, no specific side chains attract each other. The dominating factor in the packing motifs is shape selection with bulges fitting into grooves (Karle, 1992; Karle et al., 1990c).

The alignment of helices is completely parallel in crystal B (Fig. 7). This must be the case because there is only 1 molecule in a triclinic cell, space group P1. Crystal C has antiparallel packing. Figure 6 shows 1 layer of parallel helices viewed down the *b* direction of space group $P2_1$. The layers directly above and below are related to the one shown by a 2-fold screw axis, which results in the antiparallel assembly. Crystal A also has an antiparallel assembly of helices (Fig. 8) that is necessitated by the symmetry elements in space group $P2_12_12_1$.

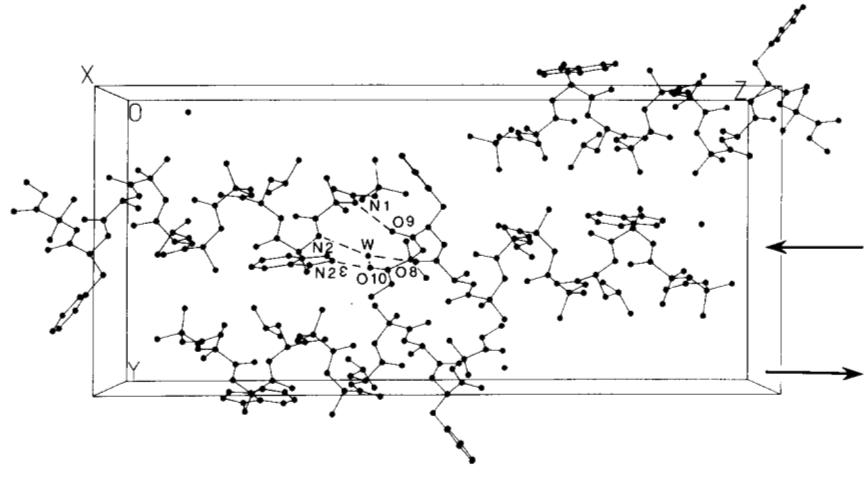

Fig. 8. Antiparallel packing of helices in crystal A. Head-to-tail hydrogen bonding is shown by dotted lines. W is the oxygen atom in a water molecule.

The variety of packing motifs and head-to-tail associations of helices shown in crystals A, B, and C does not appear to influence the formation of 3_{10}- or α-helix type. In the structures shown in this paper, only the length of the sequence is correlated with helix type.

Spectroscopic distinctions between helix types

Distinctions between 3_{10}- and α-helical conformations in short peptides cannot be easily achieved by CD methods in solution (Sudha et al., 1983). More recently, nonsequential rotating frame nuclear Overhauser effects between amide protons have been used to establish a 3_{10}-helical structure in an 8-residue peptide containing 6 Aib residues (Basu & Kuki, 1993). However, it has been noted that a full set of NOE correlations may be difficult to establish in many short peptides as a consequence of incomplete helicity. Fourier transform infrared spectroscopy (FTIR) has been advanced as a more readily applicable method for distinguishing the 2 helix types, with the amide I band of 3_{10}-helices occurring at 1,662–1,666 cm^{-1}, whereas the corresponding band in α-helical segments has been assigned at 1,657–1,658 cm^{-1} (Kennedy et al., 1991). The availability of 3 crystallographically characterized peptide helices permits an evaluation of this approach.

Figure 9 shows the partial IR spectra (N-H stretch, amide A 3,200–3,500 cm^{-1} and CO stretch, amide I, 1,600–1,700 cm^{-1}) of peptides A–C and 2 shorter fragments, Boc-Aib-Ala-Leu-Aib-Ala-Phe-Aib-OMe (D) and Boc-Ala-Leu-Aib-Ala-Phe-Aib-OMe (E), in the solid state (see Table 5). In all cases, the intense hydrogen bonded NH stretch (3,310 cm^{-1}) is consistent with the formation of helices. An interesting feature of the spectra in KBr pellets is the distinct shift to lower frequencies of the νCO band with increasing peptide chain length. Although the position of 1,667 cm^{-1} in the 6- and 7-residue peptides corresponds well to the values reported for 3_{10}-helices, the values of 1,656–1,657 cm^{-1} in the 9- and 10-residue peptides are closer to the values expected for α-helices (Kennedy et al., 1991). The intermediate band position of 1,661 cm^{-1} in the octapeptide may result from population of both types of conformations. Although X-ray analysis of single crystals establishes a clear transition between the 9- and 10-residue peptides, the IR results support a structural transition at the level of the 8-residue peptide. Differences between the 2 methods may be expected because polycrystalline samples have been used for IR measurements. Earlier crystallographic studies have already established changes in the relative amounts of 3_{10}- and α-helical conformations in mixed helices of peptides in different polymorphic forms (Karle & Balaram, 1990; Karle et al., 1990b).

Table 5. *IR band positions (cm^{-1}) for the peptides in the solid state*[a]

Peptide[b]	νNH (bonded)	νNH (free)	νCO
A(10)	3,309	3,471	1,656
B(9)	3,314	3,476	1,657
C(8)	3,316	3,424	1,661
D(7)	3,326	3,433	1,667
E(6)	3,326	3,426	1,667

[a] All spectra are recorded in KBr pellets.

[b] Peptide sequences are A, Boc-Aib-Trp-Leu-Aib-Ala-Leu-Aib-Ala-Phe-Aib-OMe; B, Boc-Trp-Leu-Aib-Ala-Leu-Aib-Ala-Phe-Aib-OMe; C, Boc-Leu-Aib-Ala-Leu-Aib-Ala-Phe-Aib-OMe; D, Boc-Aib-Ala-Leu-Aib-Ala-Phe-Aib-OMe; E, Boc-Ala-Leu-Aib-Ala-Phe-Aib-OMe.

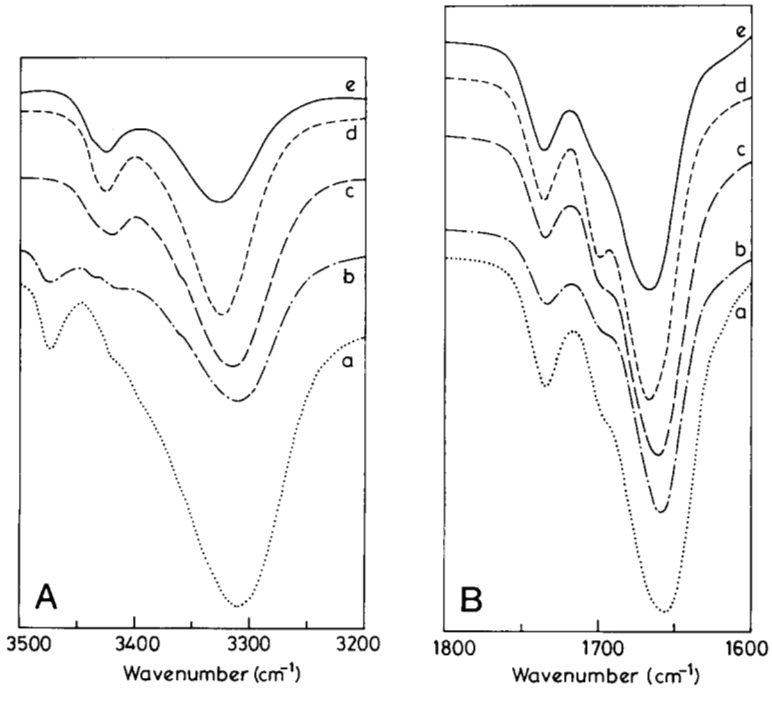

Fig. 9. FTIR spectrum in KBr pellets of the peptides. **A:** The amide A (νNH) region. **B:** The amide I (νCO) region. a, Boc-Aib-Trp-Leu-Aib-Ala-Leu-Aib-Ala-Phe-Aib-OMe; b, Boc-Trp-Leu-Aib-Ala-Leu-Aib-Ala-Phe-Aib-OMe; c, Boc-Leu-Aib-Ala-Leu-Aib-Ala-Phe-Aib-OMe; d, Boc-Aib-Ala-Leu-Aib-Ala-Phe-Aib-OMe; e, Boc-Ala-Leu-Aib-Ala-Phe-Aib-OMe.

Discussion

In the present study, chain-length factors appear to determine the 3_{10}- to α-helical structural transition, as suggested earlier for alternating $(Aib\text{-}Ala)_n$ sequences on the basis of crystallographic analysis (Pavone et al., 1990a) and for related $(Ala\text{-}Aib)_n$ sequences (Otoda et al., 1993). In NMR studies of octapeptides containing 6 Aib residues and 2 internal aromatic amino acids, sequence permutation has been reported to induce a structural transition (Basu et al., 1991). Indeed, NMR studies of heptapeptides with $(X\text{-}Aib)_n$ sequences have suggested the possibility of solvent-induced structural transitions (Vijayakumar & Balaram, 1983). Clearly, in moderately sized peptides, energetic barriers for 3_{10}- to α-helical transitions are small and can be easily traversed under a variety of experimental conditions. Recent theoretical analyses evaluating energetics of 3_{10}-/α-helical transitions in short peptides (Rives et al., 1993; Smythe et al., 1993; Huston & Marshall, 1994) suggest that carefully designed experiments may be necessary to clarify the factors determining the transition between closely related helical structures in peptides.

Materials and methods

The model peptides were synthesized by a conventional solution-phase procedure with a fragment condensation approach (Balaram et al., 1986) and purified by reverse-phase high-performance liquid chromatography (C_{18}, 10 μ, methanol–water gradient). Crystals of A, B, and C were grown by slow evaporation from CH_3OH/H_2O solution, isopropanol/H_2O solution, and CH_3OH/H_2O solution, respectively. Infrared spectra (KBr pellets) were recorded on a BioRad FTS-7 spectrometer equipped with an SPC-3200 computer.

X-ray diffraction data for each peptide were collected with CuKα radiation on an automated 4-circle diffractometer with

Table 6. *Crystal and diffraction data*

	C[a]	B[a]	A[a]
Molecular formula	$C_{45}H_{74}N_8O_{11}\cdot 2H_2O\cdot CH_3OH$	$C_{56}H_{84}N_{10}O_{12}$	$C_{60}H_{91}N_{11}O_{13}\cdot H_2O$
Crystallizing solvent	CH_3OH/H_2O	$isoC_3H_7OH/H_2O$	CH_3OH/H_2O
Molecular weight	903.14 + 68.08	1,089.36	1,174.46 + 18.02
Crystal size (mm)	0.15 × 0.20 × 0.35	0.30 × 0.34 × 0.09	0.20 × 0.30 × 0.05
Space group	$P2_1$	P1	$P2_12_12_1$
a (Å)	16.211(3)	9.372(2)	10.604(2)
b (Å)	11.320(2)	10.411(2)	17.072(4)
c (Å)	16.636(3)	16.740(3)	37.308(9)
α (deg)	90.	73.15(2)	90.
β (deg)	109.54(2)	82.95(2)	90.
γ (deg)	90.	81.30(2)	90.
Volume (Å^3)	2,877.0(9)	1,539.9(5)	6,754(3)
Z	2	1	4
d_{calc} (g cm^{-3})	1.121	1.174	1.172
Scan speed (deg/min)	8.0–15.0	9.8	6
Max 2θ (deg)	112	112	112
Resolution (Å)	0.93	0.93	0.93
hkl range	*h*, −17 → 16; *k*, 0 → 12; *l*, 0 → 17	*h*, −9 → 10; *k*, 0 → 11; *l*, −17 → 18	*h*, 0 → 11; *k*, −18 → 0; *l*, 0 → 40
Radiation, λ (Å)	1.54178	1.54178	1.54178
Temperature (K)	293	293	293
Total no. independent data	3,990	4,284	4,948
No. with $\lvert F_o\rvert > 3(\sigma)(F)$	3,004	3,810	2,735
No. parameters refined	613	732	754
Ratio no. parameters/no. data	4.9:1	5.2:1	3.7:1
Final *R*, R_w (%)[b]	7.3, 6.9	5.4, 5.9	8.3, 5.7
Goodness of fit[c]	1.90	1.88	1.34
Maximum difference (*e*/Å)[d]	0.28	0.26	0.31
Minimum difference (hole) (*e*/Å)[d]	−0.22	−0.28	−0.29

[a] Numbers in parentheses represent estimated standard deviations.

[b] $$R = \frac{\sum |(F_{obs} - F_{calc})|}{\sum |(F_{obs})|} = \frac{\sum (del)}{\sum (F_{obs})} \qquad R_w = \frac{\sum (del \cdot w^{1/2})}{\sum (F_{obs} \cdot w^{1/2})},$$

where $w = [\sigma^2(F) + gF^2]^{-1/2}$.

[c] Goodness of fit = s = $$\left[\frac{\sum (w \cdot del^2)}{(M - N)}\right]^{1/2},$$

where M = no. of observed reflections and N = no. of parameters refined.

[d] Maximum and minimum heights in final difference map.

a graphite monochromator (Nicolet R3). Three reflections used as standards, monitored after every 97 measurements, remained constant within 3% during the data collection for each of the 3 crystals. Cell parameters and other diffraction data are shown in Table 6. The structures were solved by direct phase determination with the use of programs contained in the SHELXTL package (Sheldrick, 1990). The locations of solvent atoms were found in difference maps. After several cycles of least-squares refinement, H atoms were placed in ideal positions on the C and N atoms and allowed to ride with the atom to which they were bonded during the remainder of the full-matrix least-squares refinement.

Fractional coordinates for the C, N, and O atoms have been deposited with the Cambridge Crystallographic Data Bank. Bond lengths (e.s.d. 0.02 Å) and bond angles (e.s.d. 1.5°) do not show significant or systematic differences from expected values.

Acknowledgments

This research was supported in part by the National Institutes of Health grant GM 30902, by the Office of Naval Research, and by a grant from the Department of Science and Technology, India. R.G. acknowledges receipt of a Senior Research Fellowship from the Council of Scientific and Industrial Research, India. The use of the infrared spectrometer at the Department of Inorganic and Physical Chemistry, IISc, is also gratefully acknowledged.

References

Balaram H, Sukumar M, Balaram P. 1986. Stereochemistry of α-aminoisobutyric acid peptides in solution. Conformations of decapeptides with a central triplet of contiguous L-amino acids. *Biopolymers 25*:2209–2223.

Barlow DJ, Thornton JM. 1988. Helix geometry in proteins. *J Mol Biol 168*:601–619.

Basu G, Bagchi K, Kuki A. 1991. Conformational preferences of oligopeptides rich in α-aminoisobutyric acid. 1. Observation of a $3_{10}/\alpha$-helical transition upon sequence permutation. *Biopolymers 31*:1763–1774.

Basu G, Kuki A. 1993. Evidence for a 3_{10}-helical conformation of an eight residue peptide from ^1H-^1H rotating frame Overhauser studies. *Biopolymers 33*:995–1000.

Bosch R, Jung G, Schmitt H, Winter W. 1985a. Crystal structure of the α-helical undecapeptide Boc-L-Ala-Aib-Ala-Aib-Ala-Glu(OBzl)-Ala-Aib-Ala-Aib-Ala-OMe. *Biopolymers 24*:961–978.

Bosch R, Jung G, Schmitt H, Winter W. 1985b. Crystal structure of Boc-Leu-Aib-Pro-Val-Aib-Aib-Glu(OBzl)-Gln-Phol·xH_2O, the C terminal nonapeptide of the voltage dependent ionophore alamethicin. *Biopolymers 24*:979–999.

Fiori WR, Miick SM, Milhauser GL. 1993. Increasing sequence length favors α-helix over 3_{10}-helix in alanine-based peptides; evidence for a length dependent structural transition. *Biochemistry 32*:11957–11962.

Francis AK, Iqbal M, Balaram P, Vijayan M. 1983. The crystal structure of a 3_{10}-helical decapeptide containing α-aminoisobutyric acid. *FEBS Lett 155*:230–232.

Francis AK, Vijayakumar EKS, Balaram P, Vijayan M. 1985. A helical peptide containing a majority of valyl residues. The crystal structure of *t*-butyloxycarbonyl-(L-valyl-α-aminoisobutyryl)$_3$-L-valyl methyl ester monohydrate. *Int J Pept Protein Res 26*:214–233.

Hol WGJ, de Maeyer MCH. 1984. Electrostatic interactions between α-helix dipoles in crystals of an uncharged helical undecapeptide. *Biopolymers 23*:809–817.

Hol WGJ, Halie LM, Sander C. 1981. Dipoles of the α-helix and α-sheet: Their role in protein folding. *Nature 294*:532–536.

Huston SE, Marshall GR. 1994. Helix transitions in methylalanine homopeptides: Conformational transition pathway and potential of mean force. *Biopolymers 34*:75–90.

Karle IL. 1992. Folding, aggregation and molecular recognition in peptides. *Acta Crystallogr B 48*:341–356.

Karle IL, Balaram P. 1990. Structural characteristics of α-helical peptide molecules containing Aib residues. *Biochemistry 29*:6747–6756.

Karle IL, Flippen-Anderson JL, Sukumar M, Balaram P. 1990a. Parallel and antiparallel aggregation of α-helices: Crystal structure of two apolar decapeptides X-Trp-Ile-Ala-Aib-Ile-Val-Aib-Leu-Aib-Pro-OMe (X = Boc,Ac). *Int J Pept Protein Res 35*:518–526.

Karle IL, Flippen-Anderson JL, Sukumar M, Balaram P. 1992a. Helix packing in peptide crystals as models for proteins. A distorted leucine ladder in the structure of a leucine rich decapeptide. *Proteins Struct Funct Genet 12*:324–330.

Karle IL, Flippen-Anderson JL, Sukumar M, Balaram P. 1992b. Differences in hydration and association of helical Boc-Val-Ala-Leu-Aib-Val-Ala-Leu-(Val-Ala-Leu-Aib)$_2$-OMe·xH_2O in two crystalline polymorphs. *J Med Chem 35*:3885–3889.

Karle IL, Flippen-Anderson JL, Uma K, Balaram H, Balaram P. 1989. α-Helix and $3_{10}/\alpha$-mixed helix in cocrystallized conformers of Boc-Aib-Val-Aib-Aib-Val-Val-Val-Aib-Val-Aib-OMe. *Proc Natl Acad Sci USA 86*:765–769.

Karle IL, Flippen-Anderson JL, Uma K, Balaram P. 1990b. Helix aggregation in peptide crystals. Occurrence of either all parallel or antiparallel packing motifs for α-helices in polymorphs of Boc-Aib-Ala-Leu-Ala-Leu-Aib-Leu-Ala-Leu-Aib-OMe. *Biopolymers 29*:1835–1845.

Karle IL, Flippen-Anderson JL, Uma K, Balaram P. 1990c. Parallel zippers formed by α-helical peptide columns in crystals of Boc-Aib-Glu(OBz)-Leu-Aib-Ala-Leu-Aib-Ala-Lys(Z)-Aib-OMe. *Proc Natl Acad Sci USA 87*:7921–7925.

Karle IL, Sukumar M, Balaram P. 1986. Parallel packing of α-helices in crystals of Boc-Trp-Ile-Ala-Aib-Ile-Val-Aib-Leu-Aib-Pro-OMe·$2H_2O$. *Proc Natl Acad Sci USA 83*:9284–9288.

Kavanaugh JS, Moo-Penn WF, Arnone A. 1993. Accommodation of insertions in helices: The mutation in hemoglobin Cantonsville (Pro 37 α-Glu-Thr 38α) generates a $3_{10} \rightarrow \alpha$ bulge. *Biopolymers 32*:2509–2513.

Keefe LJ, Sondek J, Shortle D, Lattman EE. 1993. The α aneurism: A structural motif revealed in an insertion mutant of staphylococcal nuclease. *Proc Natl Acad Sci USA 90*:3275–3279.

Kennedy DF, Crisma M, Toniolo C, Chapman D. 1991. Studies of peptides forming 3_{10}- and α-helices and β-bend ribbon structures in organic solution and in model biomembranes by Fourier transform infrared spectroscopy. *Biochemistry 30*:6541–6548.

Marshall GR, Hodgkin EE, Langs DA, Smith DG, Zabrocki J, Leplawy MT. 1990. Factors governing helical preference of peptides containing multiple α,α-dialkyl amino acids. *Proc Natl Acad Sci USA 87*:487–491.

Miick SM, Martinez GV, Fiori WR, Todd AP, Milhauser GL. 1992. Short alanine based peptides may form 3_{10}-helices and not α-helices in aqueous solutions. *Nature 359*:653–655.

Otoda K, Kitagawa J, Kimura S, Imanishi Y. 1993. Chain length dependent transition of 3_{10} to α-helix of Boc(Ala-Aib)$_n$-OMe. *Biopolymers 33*:1337–1345.

Pavone V, Benedetti E, DiBlasio B, Pedone C, Santini A, Bavoso A, Toniolo C, Crisma M, Sartore L. 1990a. Critical main chain length for conformational conversion from 3_{10}-helix to α-helix in polypeptides. *J Biomol Struct Dyn 7*:1321–1331.

Pavone V, DiBlasio B, Santini A, Benedetti E, Pedone C, Toniolo C, Crisma M. 1990b. The longest regular polypeptide 3_{10} helix at atomic resolution. *J Mol Biol 214*:633–635.

Prasad BVV, Balaram P. 1984. The stereochemistry of α-aminoisobutyric acid containing peptides. *CRC Crit Rev Biochem 16*:307–347.

Richardson J. 1981. The anatomy and taxonomy of protein structure. *Adv Protein Chem 34*:167–339.

Rives JT, Maxwell DS, Jorgenson WJ. 1993. Molecular dynamics and Monte Carlo simulations favor the α-helical form for alanine based peptides in water. *J Am Chem Soc 115*:11590–11593.

Sheldrick GM. 1990. *SHELXTL*. Madison, Wisconsin: Siemens Analytical Instruments.

Smythe ML, Huston SE, Marshall GR. 1993. Free energy profile of a 3_{10}- to α-helix transition of an oligopeptide in various solvents. *J Am Chem Soc 115*:11594–11595.

Sudha TS, Vijayakumar EKS, Balaram P. 1983. Circular dichroism studies of helical oligopeptides. Can 3_{10} and α-helical conformations be chiroptically distinguished? *Int J Pept Protein Res 22*:464–468.

Toniolo C, Benedetti A. 1991. The polypeptide 3_{10} helix. *Trends Biochem Sci 16*:350–353.

Vijayakumar EKS, Balaram P. 1983. Solution conformation of penta and heptapeptides containing repetitive α-aminoisobutyryl-L-alanyl and α-aminoisobutyryl-L-valyl sequences. *Tetrahedron 39*:2725–2731.

Wada A. 1976. The α-helix as an electric macro-dipole. *Adv Biophys 9*:1–63.